Oxygen Adsorption by Single-Walled Carbon Nanotubes

B. G. Demczyk*

Department of Physics and Materials Science and Engineering

University of California

Berkeley, CA 94720-7300

ABSTRACT

Evidence is presented for oxygen adsorption on single walled carbon nanotubes. Furthermore, such results were not found in the case of multi wall tubes under the same experimental conditions. These results correlate well with transport measurements on single walled carbon nanotubes, which display density of states effects. We suggest a phenomenological model for this adsorption, based on simple diffusion of oxygen through individual graphene sheets.

Introduction:

The high surface area of carbon nanotubes and their hollow geometry render these materials prime candidates for use in gas storage devices. [1]. In addition, the high curvature of carbon nanofibers confers a higher surface area per given volume (or projected area) in single walled versus multi-walled carbon nanotubes. Therefore, it is expected that, for a given volume of tubes, a higher percentage of oxygen, a higher oxygen per volume of tubules, would be present in the single walled case. Transport measurements, as well as scanning tunneling spectroscopy studies on single-walled carbon nanotubes have displayed conductivity and thermodynamic properties differences in single walled carbon nanotubes [2], prepared by laser-ablation techniques. In fact, it has been possible, upon exposure to oxygen to convert a semiconducting nanotube into a conducting (metal) through such exposure [3]. These results have been interpreted in terms of a "diffusing" of the density of states, due to the presence of oxygen [2]. To this point, however, no experimental verification of the presence of oxygen in these materials has been given. In this work, we have employed electron energy loss spectroscopy, associated with a transmission electron microscope to address this issue.

Experimental:

Single-walled carbon nanotubes were prepared by laser ablation, using established procedures [4]. Samples were "purified" to remove amorphous carbon and residual catalyst particles via treatment by HNO_3, followed by vacuum filtering. The dried powder

was then ultrasonically dispersed in isopropanol and deposited onto a 3 mm holey carbon-coated copper mesh grid. These grids were then examined in a JEOL 200CX transmission electron microscope (TEM), operating at 120 kV, to reduce electron beam damage to the nanotubes. The instrument was interfaced to a Gatan Model 666 parallel electron energy loss spectrometer (PEELS), with which oxygen levels were detected. All PEELS work was performed in the image coupling mode, using a 3mm slit *a*nd 240 μm selected area diffraction aperture, at a collection angle of 80 mrad, which is optimal collection angle for the oxygen peak at this electron beam energy [5]. In-situ heating was performed, using a Gatan model 628 heating (tantalum furnace) holder.

Results:

Most single-walled tubes occurred in the form of bundles (Figure 1), although occasional isolated single tubes could be found (Figure 2). The latter were extremely electron beam sensitive, however, and unsuitable for spectroscopic analysis. Consequently, a bundle of tubes was analyzed. Figure 3a shows the PEELS spectrum for such a group of nanotubes, collected over a period of 200 seconds at a beam intensity (approx. 60 pA), pixel sampling (0.5 A/pixel) and dwell time (0.05 s/pixel), chosen to maximize the EELS signal while ensuring minimal ionization damage. Spectral features include the predominant C kalpha edge at 284 eV, plus smaller peaks at 465 and 532 eV. An expanded portion of this portion of the spectrum is shown in Figure 3b, and shows the 532-eV peak, due to oxygen. Figure 3b shows a complementary curve, collected under the same conditions on an adjoining portion of the carbon support grid. As shown in the inset, only the peak due to Ti is discernible above the background C k_α edge. Figure 4 was collected on the same group of carbon nanotubes at a temperature of 225 C. As shown in the inset, the oxygen peak has receded into the background, indicating that any

oxygen present has having desorbed from the surface (or diffused through the walls of the nanotubes). We have quantified these spectra, using the Gatan EL/P software package. Backgrounds were modeled, using an exponential fit over a window 80 eV in front of the oxygen peak of interest. This same modeled background was then utilized for the cases where no discernible oxygen peak was present, as well. O/C ratios were computed to be 0.057 ± 0.009 and 0.024 ± 0.004 for the tube bundle before and after 15 minutes of heating. For reference, the O/C ratio for the adjacent holey carbon region was found to be 0.043 ± 0.008, prior to heating. These values illustrate the difficulties involved in attempting quantification at such low oxygen levels. It is reasonable that some oxygen resides on the surface of the carbon support film and on the tube bundle, (subsequent to heating), even though they are not detectable above background in the PEELS spectra of Figures 3b and 3c. Taking the holey carbon grid spectrum as our "zero" point, i.e. the point at which the oxygen energy loss peak recedes into the background, we can reasonably say that at least 1.4% of oxygen is lost from the tube bundle upon heating. We should also note that we have attempted to detect oxygen on groups of multiwall carbon nanotubes under similar collection conditions and have found none (Figure 5). This suggests that oxygen adsorption to single wall tubes may be facilitated by defects and/or that oxygen may diffuse through the single wall and accumulate in the core of the individual tubes. If the desorption is strain induced, bound of stability due to the higher radius of curvature of single versus multiple walled tubes. Laue et al. have calculated carbon binding energy for molecular oxygen affinity on structured single wall tubes as 3 eV (ref 3). Clearly, oxygen diffusion through a single graphene layer is more probable than through a succession of concentric tube walls? It is also possible that oxygen enters single wall tubes through open end regions, which are more common in the single wall

rather than multiwall case. Since the EELS technique samples, the thickness of the entire nanotube bundle, it is not possible to distinguish between these two effects.

Discussion:

The (one dimensional) diffusion of oxygen through a graphene sheet is governed by Fick's first and second laws, of the form: $dC(x,y)/dt = D\, d^2(x,t)/dx^2$,

$J = -Ddc/dv$, and $dc/dt = D\, d^2c/dx^2$

where:

J is the diffusion flux, D, the diffusion coefficient, c, the concentration and x, the position

For the diffusion width, the boundary conditions (constant concentration source and diffusion length):

$c(0, t) = c_0$; $c(\infty, t) = 0$

And with the initial condition; $c(x,0) = 0$

The concentration is governed by the following relation [6]:

$C(x,,t) = Co\ \mathrm{erfc}\ (x/2\pi\ (Dt)^{0.5})$, where erfc is the complementary error function (= 1 – erf, the error function).

Now, allowing a very long time for diffusion in the nanotube case, ($t \rightarrow \infty$). Now for $t \rightarrow \infty$)., $\mathrm{erfc}\ (0) = 0.7$ [7]. Thus, for a single wall tube, $c(x, \infty)) = 0.77\ c_o$. For a 10-wall tube, however, erfc $c(\infty) = 0.073\ c_0$, less than one tenth of the single walled case.

We can also see, however, that after some period, an equilibrium concentration is reached, after which the driving force for further diffusion will be reduced.

Since the resultant concentration on the interior of the graphene sheet is lower than the original concentration external to the nanotube, one can see that the driving force for diffusion through additional walls is less, Therefore, the probability of oxygen diffusing to the interior of multiple-walled tubes is reduced. This manifests itself in lower (i.e., negligible above background) O/C ratios observed in multiple walled tubes.

Diffusion can also occur through multiple wall end cap effects (there are no end caps in single walled carbon nanotubes. Also, there is a reduced number of defects in the single walled case. This manifests itself in the lower (i.e., negligible above background) O/C rations observed in multiple walled tubes.

Summary:

We have found evidence for oxygen absorption of the surface of single-walled carbon nanotubes, prepared by laser ablation. These results are consistent with transport measurements reported elsewhere, this oxygen is desorbed upon heating. These results suggest possible application as reversible gas sensing and storage devices.

Acknowledgements

Sincere appreciation is extended to professors A. Zettl and R. O. Ritchie, of the Department of Physics and Materials Science and Engineering, respectfully of the University of California, Berkeley for their supprrt of this work. Samples were synthesized by R. Sivamani, under supervision of J. Cumings. Transmission electron microscopy was performed at the National Center for Electron Microscopy, Berkeley, CA. This research was funded, in part, by the Director of the Office of Energy Research, Office of Basic Energy Sciences, Materials Sciences Division of the United States Department of Energy, contract number DEAC03-76SF00098.

References:

[1] A. Rubio, J. Corkill and M. L. Cohen, Phys. Rev. Lett. 49, 5081 (1994).

[2] P.C. Collins, K. Bradley, M. Ishigami and A. Zettl, Science 287, 1801 (2000).

[3] P.C. Collins. M. Ishigami and A. Zettl, in "Cluster and Nano", World Scientific, p.411, (2000).

[4] X. Blase, A. Rubio, S. G. Louie and M. L. Cohen, Europhys. Lett. 28, 335 (1994).

[5] P.M. Budd and P. J. Goodhew, "Light Element Analysis in the Transmission Electron Microscope: WEDX and EELS", Royal Microscopical Society Handbook No. 16; Oxford University Press 1988, pp 48-55.

[6] P. G. Shewmon, "Diffusion in Solids", 2nd Edition., The Minerals, Metals and Materials Society, Warrendale, PA, pp. 22-23, 1989.

[7] see, for example, https://www.montana.edu/tjkaiser/ee407/notes/comperrfnc.pdf.

List of Figures

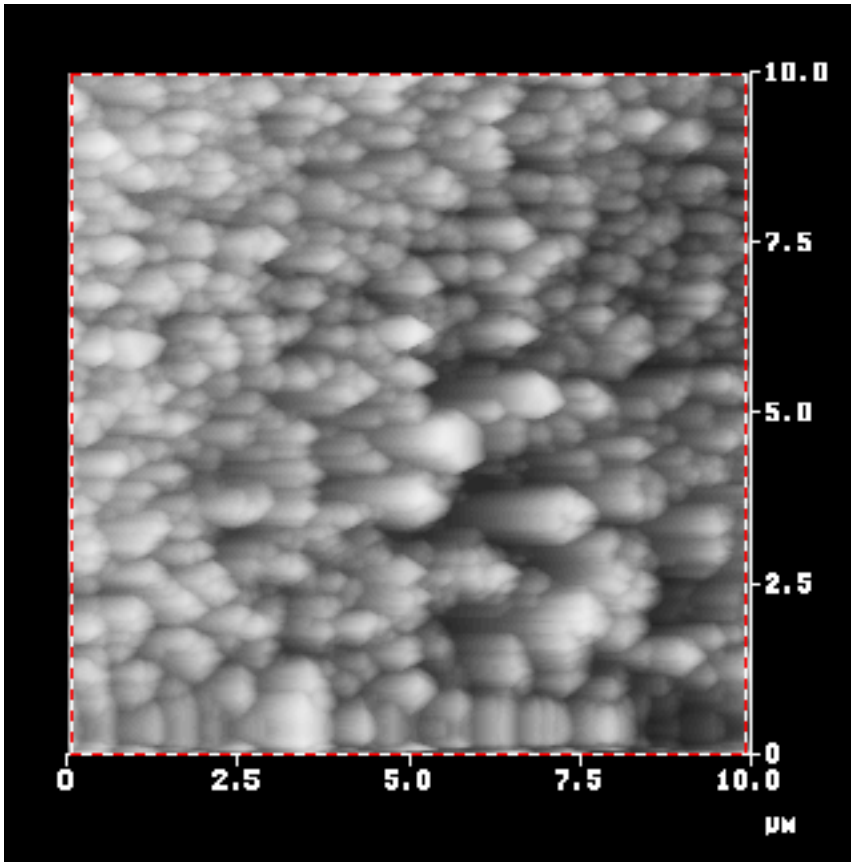
10.0
7.5
5.0
2.5
0
0
2.5
5.0
7.5
10.0
μm

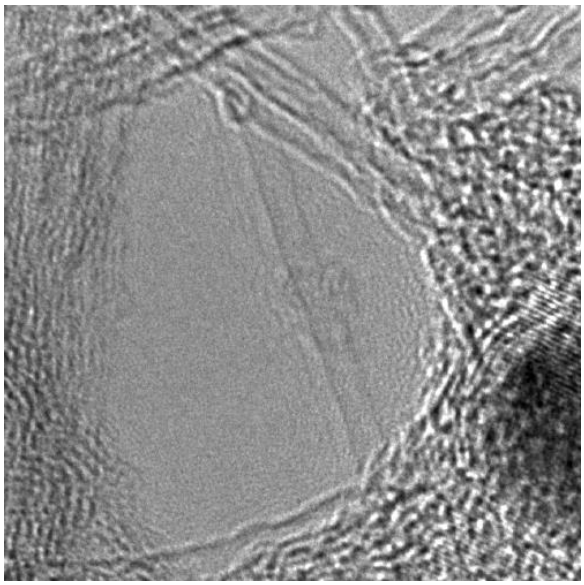

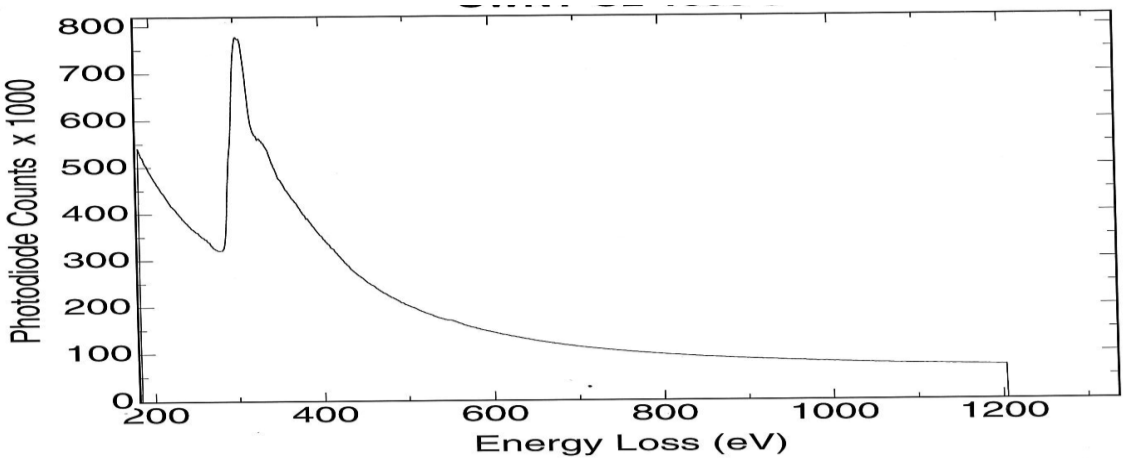
Photodiode Counts x 1000
800
700
600
500
400
300
200
100
0
200
400
600
800
1000
1200
Energy Loss (eV)

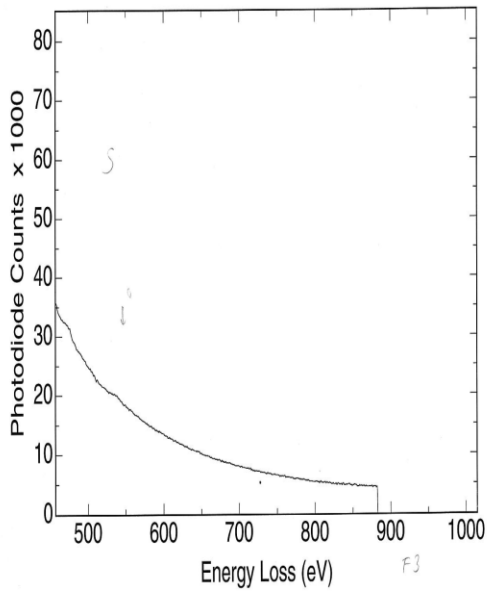
Photodiode Counts x 1000
80
70
60
50
40
30
20
10
0
500
600
700
800
900
1000
Energy Loss (eV)

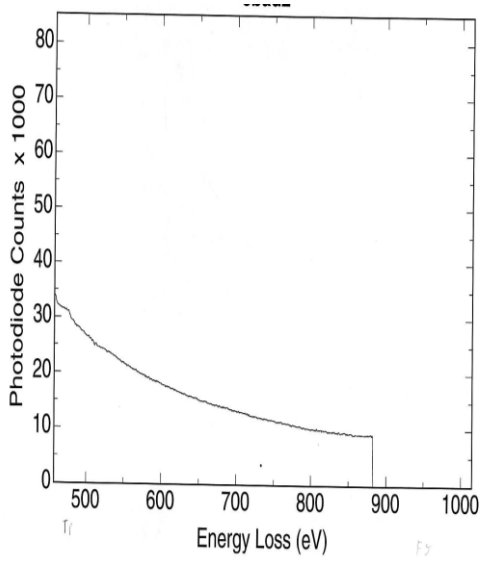
Photodiode Counts x 1000
80
70
60
50
40
30
20
10
0
500
600
700
800
900
1000
Energy Loss (eV)

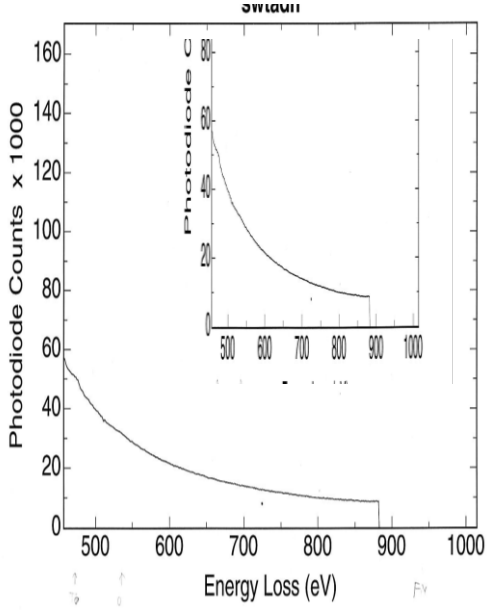
Photodiode Counts x 1000
160
140
120
100
80
60
40
20
0
500
600
700
800
900
1000
Energy Loss (eV)